January 1991

A Search for Embedded Young Stellar Objects in and near the IC 1396 Complex

Richard Schwartz
University of Missouri

Bruce Wilking
University of Missouri–St. Louis

Armen Giulbudagian

THE ASTROPHYSICAL JOURNAL, 370:263–271, 1991 March 20

A SEARCH FOR EMBEDDED YOUNG STELLAR OBJECTS IN AND NEAR THE IC 1396 COMPLEX

RICHARD D. SCHWARTZ
Department of Physics, University of Missouri-St. Louis, 8001 Natural Bridge Road, St. Louis, MO 63121

ARMEN L. GYULBUDAGHIAN
Byurakan Astrophysical Observatory, Armenian S.S.R., U.S.S.R.

AND

BRUCE A. WILKING[1]
Department of Physics, University of Missouri-St. Louis, 8001 Natural Bridge Road, St. Louis, MO 63121
Received 1990 July 27; accepted 1990 September 11

ABSTRACT

The *IRAS* data base is used to locate young stellar object candidates in and near the IC 1396 complex located in the Cepheus OB2 association. Co-added survey data are used to identify all sources with a flux density $S_\nu(100) > 10$ Jy and with $S_\nu(100) > S_\nu(60)$. The 15 sources located at the positions of globules and dark clouds are further analyzed using the inscan slices to assess the source profiles. Estimates of heating caused by OB stars in the complex are made at each source location. Six globule-related sources are found to have pointlike structure, and luminosities considerably in excess of that which can be caused by external heating. A list of 24 additional sources, unrelated to dark cloud structures, is presented along with source fluxes, luminosities, and external heating estimates.

Subject headings: infrared: sources — nebulae: H II regions — nebulae: individual (IC 1396) — stars: pre–main-sequence

1. INTRODUCTION

The Cep OB2 group of loosely-clustered OB stars has been the focus of recent studies by Kun, Balázs, & Toth (1987), Kun & Balázs (1987), and Balázs & Kun (1989). Using *IRAS* Sky Flux images, Kun et al. (1987) found evidence for a giant infrared bubble centered near $l = 102.^\circ8$, $b = +6.^\circ7$, with a diameter of about 7°. Several H II regions, including IC 1396, S129, S133, S134, and S140, are apparently associated with the expansion of this bubble which may have originated from a supernova explosion two to three million years ago.

One of the youngest and most active H II regions in the group is IC 1396. The nebula exhibits a well-defined ringlike structure about 3° in diameter, and it is excited by an O6 star (HD 206267) and a group of B stars (the cluster Trumpler 37). At a distance of about 750 pc, IC 1396 is rich in sharp-rimmed dust clouds and globules indicative of regions with ongoing star formation. Although the Cep OB2 region and IC 1396 have received a thorough analysis regarding their (OB) stellar content (e.g., Simonson 1968), detailed radio and infrared studies of molecular cloud features have been somewhat limited with emphasis upon the bright-rimmed clouds A and B (Pottasch 1956) located immediately west of the O star (e.g., see Matthews 1979; de Muizon et al. 1980; and Wootten et al. 1983). Kun (1986) has reported the detection of 155 Hα emission stars in IC 1396 which signals the presence of young stars. Marschall, Comins, & Karshner (1990) have obtained UBV photometry of 120 stars in IC 1396, and a number of pre–main-sequence candidate stars correlate with stars from Kun's (1986) sample.

Gyulbudaghian (1985) has carried out a survey of Cep OB2 in which at least two radial systems of globules (GRS) have been identified at and near IC 1396. One system, consisting of 16 globules, is centered on IC 1396, whereas the second system of 12 globules appears possibly to be associated with BD + 55 2612, a star located about 2.°2 SSE of HD 206267. The former system is dominated by bright-rimmed structures with diffuse tails generated by the radiation field from HD 206267. The latter system appears as opaque globules without bright rims (i.e., without surrounding H II emission), but with trailing structures opposite the direction to BD + 55 2612, a probable evolved A-type supergiant. The detection of H I throughout the second radial system (Simonson & van Someren Greve 1976) suggests that it may be a relic of an old H II region. The second system partially overlaps the IC 1396 system, and the second system is probably largely in the foreground of IC 1396. Gyulbudaghian, Rodriguez, & Canto (1986) have also surveyed the GRS globules for CO emission. Out of 32 globules, 26 were detected in ^{12}CO, and 17 in ^{13}CO. Moreover, the two radial systems of globules are separated in velocity space with the HD 206267 system showing a mean LSR velocity of -2.8 ± 2.4 km s^{-1}, and the BD + 55 2612 system showing a mean LSR velocity of $+6.5 \pm 1.0$ km s^{-1}. Two of the globules, GRS 12 and GRS 14, are also associated with H_2O masers (Gyulbudaghian, Rodriguez, & Curiel 1990).

In this paper we report the results of an analysis of *IRAS* co-added survey data around the IC 1396 complex to study the correlation of infrared sources with GRS globules and related cloud structures. The purpose of the study is to identify sites of probable star formation as a guide to future observational work.

2. ANALYSIS OF *IRAS* SOURCES

2.1. *The Point Source Catalog*

Embedded young stellar objects (YSOs) have been shown to produce characteristic *IRAS* color indicies as defined in the

[1] Guest investigator at the Image Processing and Analysis Center which is funded by NASA as part of the *IRAS* extended mission program under contract to JPL.

studies of Wouterloot & Walmsley (1986) and Emerson (1988). For deeply embedded sources which exhibit no optical counterparts, one generally finds flux densities $S(100\ \mu m) > S(60\ \mu m) > S(25\ \mu m) > S(12\ \mu m)$, indicative of low-temperature (<60 K) emission. The situation is complicated by the fact that other types of sources, for example the cores of galaxies and infrared cirrus, can show similar colors, so *IRAS* colors alone are not sufficient for the identification of embedded YSOs.

As a first reconnaisance for embedded YSOs in the IC 1396 complex, a region bounded by the coordinates 21^h25^m–21^h51^m, 55°30′–58°49′ (central galactic coordinates $l = 99.^\circ3$, $b = 3.^\circ6$) was scanned in the *IRAS* Point Source Catalog (Version 2 1988, hereafter PSC) for all sources with $S(100\ \mu m) > 10$ Jy and with detections in at least two other *IRAS* bands. Control areas, each of equal area (9.4 deg^2) were chosen at the same galactic latitude but at nearby galactic longitudes which are free of obvious dark cloud structures and H II regions. The IC 1396 region yielded 49 sources, control area 1 ($l = 88.^\circ5$, $b = 3.^\circ7$) contained 14 sources, and control area 2 ($l = 108.^\circ6$, $b = 3.^\circ3$) contained 17 sources. Among the 49 sources in the IC 1396 scan, it is possible to eliminate at least five sources upon the basis of identifications with visible stars or other objects which are unrelated to IC 1396. IRAS 21419+5832, for example, is identified with the M2Ia star μ Cep. The source 21306+5540 is identified with the Sharpless object S128 which is a distant (~8 kpc) compact H II region. A faint H II region appears at the position of 21306+5532. The source 21318+5631 has colors indicative of an OH/IR star (Olnon et al. 1984), hence it is probably an evolved star unrelated to IC 1396, and 21329+5647 is identified in the PSC as a carbon star. The control area scans suggest a background component of about 15 sources, thus roughly 30 PSC sources appear to be indigenous to IC 1396.

2.2. *IRAS COADD and ADDSCAN/SCANPI Analyses*

Given the complexity of far-infrared emission in extended H II regions with extensive dark cloud structure, it is useful to examine both the intensity and flux (two-dimensional) contour plots of IC 1396 afforded by *IRAS* co-added survey data through the IPAC COADD product (IPAC User's Guide 1989). A montage of four co-added 60 μm intensity plots covering IC 1396 is presented in Figure 1 (Plate 16). For comparison, the optical image of the complex obtained by Osterbrock (1957) is shown in Figure 2 (Plate 16). Much of the dark cloud structure outlined by bright rims in the optical picture is evident in the extended 60 μm emission in Figure 1. The central portion of the H II region has apparently been evacuated of dust by the exciting O star as indicated by the paucity of 60 μm emission in an oblong cavity containing the star.

The co-added flux data have been used to identify embedded sources in IC 1396. The COADD template permits the identification of point sources up to 3 times fainter than found in the PSC in regions of low source density. This is especially important for the 12 and 25 μm bands where the PSC often registers only upper limits on flux densities for faint embedded sources. The threshold detection lists for each of the four bands and for each of four 2° × 2° regions covering IC 1396 have been examined for embedded sources. Three criteria were applied for the selection of sources. First, detection in all four bands was required with the position of maximum flux in each band within 50″ of one another for a given source. Second, only sources with $S(100\ \mu m) \geq S(60\ \mu m)$ were selected as potentially representative of embedded YSOs. Finally, it is well-known that infrared cirrus fluctuations can mimic cold point sources. At the distance (750 pc) of IC 1396, the general interstellar radiation field could heat a clump of dust 1′ in diameter, providing a flux $S_\nu(100\ \mu m) \sim 8$ Jy (Draine & Anderson 1985) which might be extracted as a cool point source by the COADD program. The source selection is therefore limited to sources with $S_\nu(100\ \mu m) > 10$ Jy.

Within regions of complex extended IR emission, the extraction of point sources by both the PSC and COADD templates can be problematic owing to the presence of complicated structure in the spatial distribution of the emission. In the first instance, we have selected those co-added sources which appear to be coincident in position with globules or other dark cloud features as the most likely YSO candidates. These sources have been subjected to ADDSCAN and SCANPI analyses (see IPAC User's Guide 1989) which provide one-dimensional source profiles and flux density measurements, respectively. Only in the instance of a true point source (as defined for each of the four *IRAS* bands) will the co-added flux density agree with the SCANPI flux density in a given band. Sources with extended emission, indicative of heating by external stars, will have SCANPI fluxes which are greater than the co-added fluxes since the SCANPI flux derives from integration under the entire profile, whereas the co-added flux arises only from that portion of the profile to which a point source template fit is achieved. The in-scan directions used by ADDSCAN for IC 1396 involved two series of scans, one from northeast to southwest, and one from southeast to northwest. Since an ADDSCAN profile represents the weighted mean of all scans across a source position, secondary profile structure located away from the source position cannot be uniquely located. Although such structure can be located as being either north or south of the co-add source position, there remains an ambiguity as to whether it is east or west of the coadd position.

Information on the globule-associated sources is contained in Table 1. Column (1) identifies the globules with GRS identifications from Gyulbudaghian (1985) and dark nebula identifications (LDN) from Lynds (1962). Column (2) gives *IRAS* source designations. Each source position (columns [2]–[4]) was determined from the average of the positions of maximum intensity for the bands of source detection in the COADD survey. Where the COADD positions differ sufficiently to cause a change from the PSC designation, a "C" is appended to the identification. Columns 5–7, 8–10, 11–13, and 14–16 list detailed information for each source in the 12, 25, 60, and 100 μm bands as derived from the COADD and SCANPI analyses. The first column for each band lists the flux density in Jy as determined from the COADD measurements, the second column lists the source width as found from the full width half-maximum (FWHM) in arcmin of the ADDSCAN source profile, and the third column lists the integrated SCANPI flux density in Jy. The source width has been determined from the relation

$$W = [W_0 - W_I]^{1/2}$$

where W_0 is the observed FWHM in the ADDSCAN profile, and W_I is the instrumental FWHM with values of 0.′76, 0.′77, 1.′39, and 2.′96, respectively for the 12, 25, 60, and 100 μm bands. ADDSCAN profiles which are indistinguishable from point source profiles are designated PS. It is known that COADD flux measurements are systematically lower than PSC listings for the same sources. To adjust the COADD

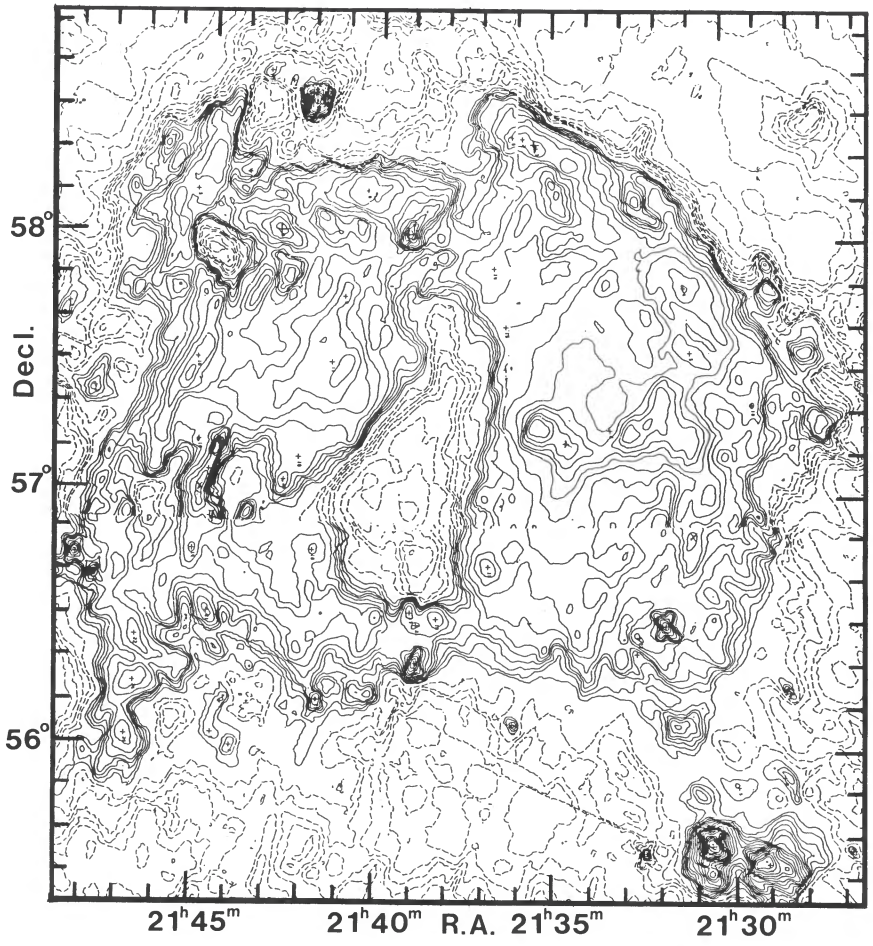

FIG. 1

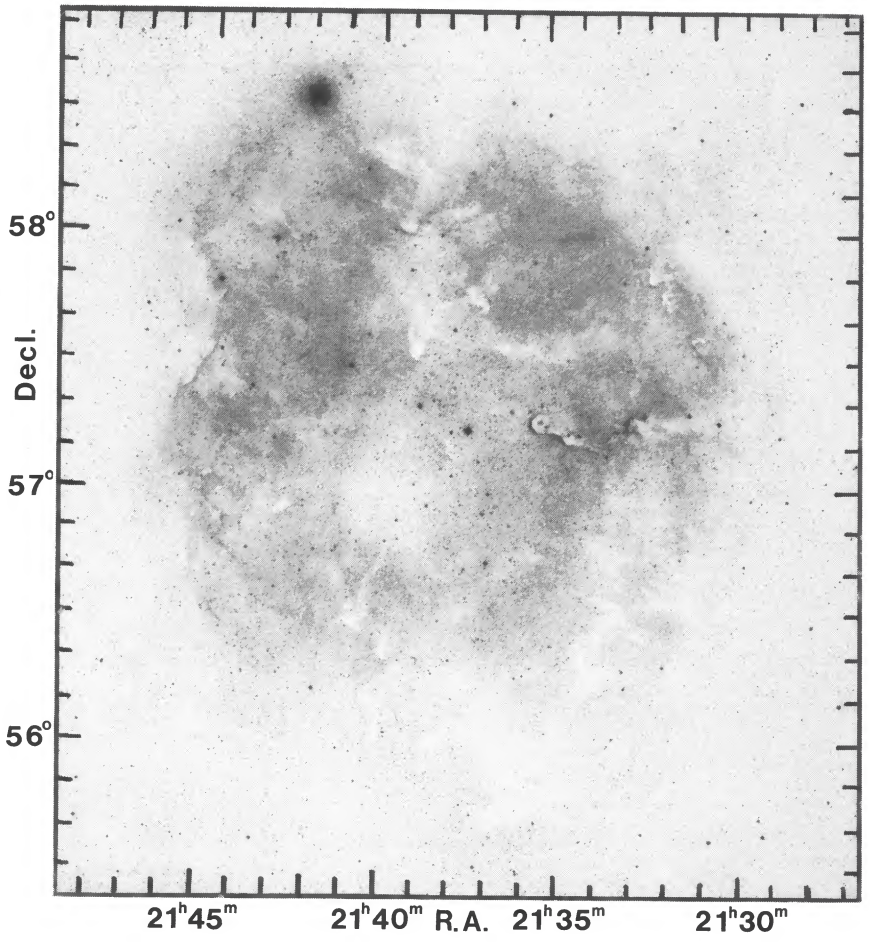

FIG. 2

FIG. 1.—*IRAS* 60 μm intensity grid for IC 1396 assembled from four 2° × 2° grids. Contour discontinuities resulting from the independently processed grids are evident at 56°52′ and at 21^h36^m.

FIG. 2.—IC 1396 region as photographed by Osterbrock (1957). The exciting O6 star HD 206267 is located at $21^h37^m.4$, 57°15′. The bright star at the upper left is μ Cep. The photograph is reproduced by permission of Lick Observatory.

SCHWARTZ, GYULBUDAGHIAN, & WILKING (see 370, 264)

TABLE 1

IRAS SOURCES ASSOCIATED WITH GLOBULES AND CLOUDS IN OR NEAR IC 1396

Globule (1)	*IRAS* Source (2)	R.A. (1950) (3)	Decl. (1950) (4)	$S_c(12)$ (Jy) (5)	$W(12)$ (′) (6)	$S_s(12)$ (Jy) (7)	$S_c(25)$ (Jy) (8)	$W(25)$ (′) (9)	$S_s(25)$ (Jy) (10)	$S_c(60)$ (Jy) (11)	$W(60)$ (′) (12)	$S_s(60)$ (Jy) (13)	$S_s(100)$ (Jy) (14)	$W(100)$ (′) (15)	$S_s(100)$ (Jy) (16)	L_c(bol) ($L_\odot$) (17)	L_c (ext. htg) (18)	L_s(bol) ($L_\odot$) (19)	L_s (ext. htg) (20)
Anon	21246+5743	38.7	14	0.25L	...	≤0.10	0.61	PS	0.73	9.7	PS	11.2	38.3:	6.7:	106.1	39	(6)	91	(6)
GRS 3	21310+5749C	05.2	50	0.20:	2.8	4.35	0.94:	3.1	9.07	13.0:	3.3	53.5	68.4	3.2	94.7	64	8	142	85
GRS 2	21312+5737C	17.3	16	0.21:	1.7	1.22	0.32:	2.2	1.53	7.2:	2.4	24.7	39.3	2.7	65.1	37	13	76	85
GRS 4	21327+5717C	43.0	17	1.03:	2.4	4.04	2.61:	2.4	7.72	35.5:	3.0	123.0	155.8:	4.1	526.5	154	19	522	239
GRS 5	21345+5818	32.2	43	0.38:	3.6	3.43	0.62:	3.6	4.55	6.6:	3.9	34.0	58.1:	6.1	256.4	51	5	240	125
GRS 6	21345+5713C	35.2	22	0.88:	2.6	4.04	1.97:	2.5	11.01	23.7:	2.5	102.8	100.3	3.4	323.2	101	41	356	357
GRS 6	21353+5717C	22.3	24	1.95:	3.8	15.62	3.07:	3.8	29.28	55.2:	4.0	247.4	273.9	3.8	593.7	263	98	743	1491
LDN 1116	21354+5822C	26.3	46	0.66:	1.4	2.64	0.89:	1.4	4.50	7.4:	3.2	40.7	41.2:	5.0	173.8	41	5	180	84
GRS 12	21388+5622	53.2	18	3.80	PS	3.61	23.24	PS	19.53	60.5	PS	62.1	81.0	PS	105.8	155	8	169	8
GRS 14	21391+5802	9.6	36	1.4:	2.7	10.07	10.73	0.8	25.45	151.6	1.1	210.4	420.1	1.4	612.9	459	9	703	14
GRS 20:	21428+5802	50.7	59	0.81:	2.2	5.20	1.31:	2.6	7.71	17.7:	3.0	40.2	115.3	2.9	181.0	106	14	198	122
GRS 23	21443+5646C	22.0	00	0.16:	1.7	0.79	0.24:	2.0	1.53	5.9	1.4	11.8	22.4	1.1	31.3	23	19	38	30
GRS 29	21445+5712	30.6	37	3.90	PS	4.32	12.63	PS	13.68	41.5	0.5	54.2	68.9	3.5	131.3	116	7	177	28
LDN 1139	21539+5821	55.2	25	0.25L	...	≤0.10	0.25L	...	≤0.05	5.7	PS	6.1	29.0	PS	31.6	~28	(2)	29	(2)
GRS 32	22051+5848	09.8	06	0.25L	0.7	1.67	5.22	PS	5.82	51.6	PS	55.3	94.0	PS	108.1	120	(1)	140	(1)

NOTE.—S_c fluxes for 21246+5743, 21539+5821, and 22051+5848 are PSC fluxes; all others are corrected COADD fluxes. A colon (:) designates poorly determined COADD fluxes.

fluxes to the PSC catalog, the ratio of PSC flux to COADD flux was determined in each band for all sources in our sample with both PSC and COADD detections. The average ratios (correction factors) were found to be 1.30, 1.44, 1.29, and 1.06, respectively, for the 12, 25, 60, and 100 μm bands. These ratios are somewhat larger than assumed in other studies, for example, that of Cohen (1990) where the reasons for the PSC-COADD flux discrepancies are discussed. The fluxes in columns (5), (8), (11), and (14) have been adjusted by our correction factors.

Bolometric luminosities have been computed for each source using both COADD and SCANPI fluxes and assuming a distance of 750 pc. The bandwidths used were 20.653, 7.538, 4.578, and 1.762 (in units of 10^{12} Hz) for the 12, 25, 60, and 100 μm bands, respectively. For cold sources a substantial fraction of the flux may fall beyond 100 μm, so the Cohen (1973) method, with Chavarria's (1981) amended constant has been used to estimate the luminosity beyond 135 μm for each source. The total bolometric luminosities L_c(bol) from the COADD fluxes and the Cohen (1973) extrapolation are contained in column (17), and the bolometric luminosities L_s(bol) from the SCANPI fluxes and the Cohen (1973) extrapolation are listed in column (19) of Table 1.

2.3. *Source Profiles and Heating Contribution from External Stars*

It is quite clear from the ADDSCAN/SCANPI analyses that most of the sources in Table 1 possess extended emission components which are probably due to heating from OB stars in the IC 1396 complex. In a number of cases, the COADD point source template has merely found "force fits" to the tops of broad profiles, usually with somewhat arbitrarily drawn baselines. Such a case is that of 21428+5802 for which the ADDSCAN profile and one-dimensional COADD point source fits for each of the four *IRAS* bands is reproduced in Figure 3*a*. In these cases the presence of a true point source is highly suspect and it is probable that the origin of the flux is due primarily to external heating. In other cases, the ADDSCAN profiles at 12 and 25 μm are consistent with the presence of two or three closely spaced sources which are not resolved in the 60 and/or 100 μm bands. It is also possible, of course, that the multiple peaks evident at 12 and 25 μm simply represent cloud structure and not the presence of unresolved point sources. An example is that of 21310+5749C which is shown in Figure 3*b*. Finally in six cases (21246+5743, 21388+5622, 21391+5802, 21445+5712, 21539+5821, and 22051+5848) it is clear that the profiles are dominated by point source-like structure. The best example is that of 21388+5622 for which the profiles are shown in Figure 3*c*. In these cases the bulk of the luminosity derives almost entirely from embedded sources.

It is possible to make coarse estimates of the heating contributions from OB stars in the complex at each *IRAS* source position, using the following assumptions:

1. The external heating of each clump is dominated by the O6 star and its close B companions (assumed combined log

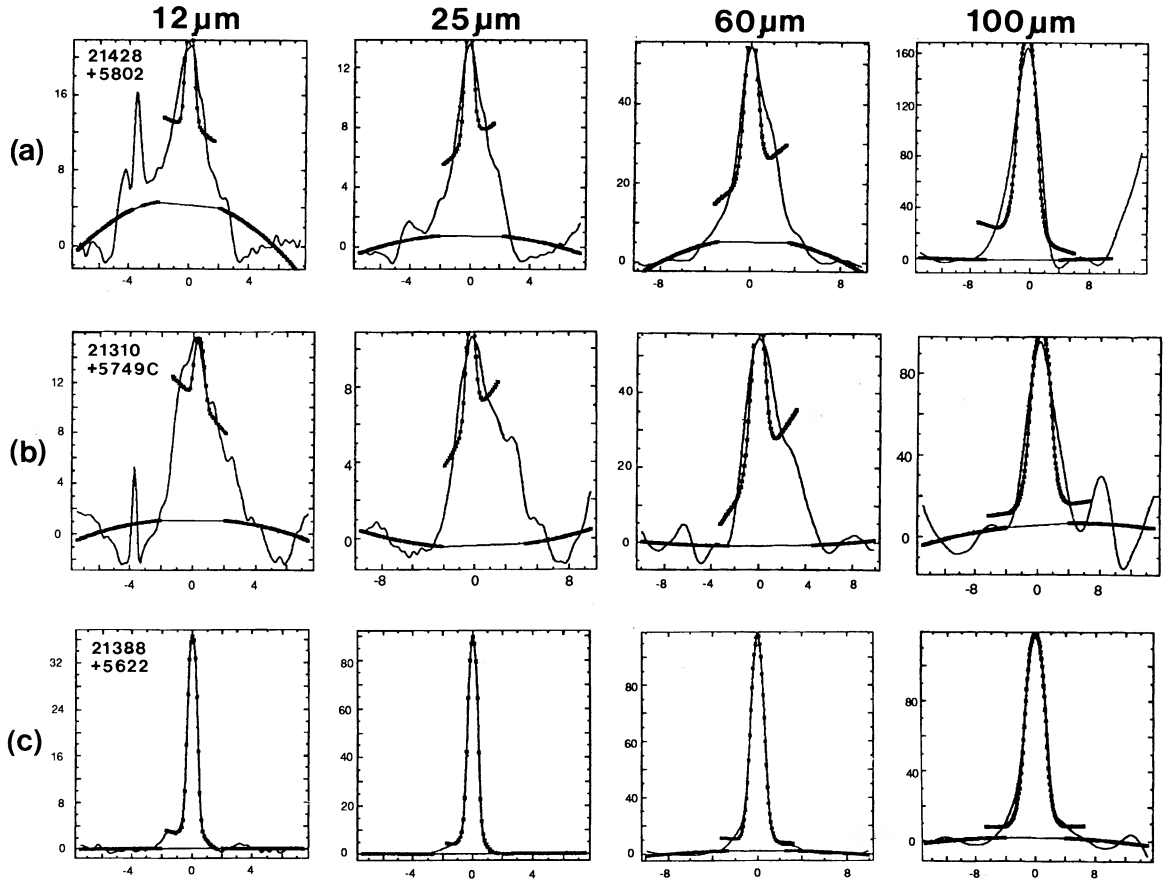

FIG. 3.—ADDSCAN profiles (*solid lines*) at 12, 25, 60, and 100 μm for the sources (*a*) 21428+5802, (*b*) 21310+5749C, and (*c*) 21366+5622. The asterisked lines are one-dimensional point source template fits and are roughly equivalent to the fits achieved in the two-dimensional COADD fits which are the bases for the S_c fluxes in Table 1. The ordinates are in units of 10^{-14} W m^{-2} per filter bandpass, and the abscissas are in arcmin.

$L = 5.73$), and 16 early B stars (B0–B3) assumed to be in the IC 1396 complex (Simonson 1968).

2. The separation of each star from each *IRAS* source is $2^{1/2}D$, where D is the projected distance between the star and the *IRAS* source assuming a distance of 750 pc to IC 1396.

3. For point source-like structure, a 1′ diameter spherical dust clump (0.22 pc at the distance of IC 1396) effectively absorbs all the radiation incident upon it from each of the OB stars, and re-emits the radiation as IR radiation. The choice of 1′ is a compromise between the higher resolution provided by the 12 and 25 μm point source templates and the lower resolution of the templates at 60 and 100 μm for which a 1′ source would appear more nearly pointlike.

4. For extended sources, the clumps are assumed to possess a width corresponding to the width (W) of each source averaged over all four bands (from columns [6], [9], [12], and [15] of Table 1).

The resultant external heating contribution for a 1′ clump appropriate for a point source [L_c(ext. htg.)] is given in column (18) of Table 1 for each source. Column (20) lists the heating values [L_s(ext. htg.)] based upon assumption 4 for extended sources. Comparison of the values L_c(bol) and L_c(ext. htg.), as well as the values L_s(bol) and L_s(ext. htg.) for each source, yields some indication of whether the source possesses substantial intrinsic heating. Sources which exhibit L(bol) $\gg L$(ext. htg.) for both the point source and extended source calculations are almost certainly dominated by embedded sources. Because of the substantial uncertainties implicit in the external heating calculations, we conservatively adopt L(bol) $> 3L$(ext. htg.) as a criterion for the presence of an intrinsic point source.

Figure 4 (Plates 17–19) presents individual charts identifying the locations of the sources in Table 1. Sources with pointlike structure are designated with a (+) sign. Extended sources are characterized by crosses representative of the average FWHM for each source and with the cross directions indicating the average of each of the two series of in-scan directions used by ADDSCAN.

2.4. *Other Sources in IC 1396*

The co-added data reveal the presence of a number of additional cold sources in IC 1396 which have no apparent association with visible cloud structures. Table 2 contains information on these sources with columns (1)–(3) as in Table 1, columns (4)–(7) presenting the flux densities in the four *IRAS* bands, column (8) listing the bolometric luminosity (L_c) computed from the COADD fluxes with the Cohen (1973) extrapolation, and column (9) the external heating contributions at each source location computed as described above. Since ADDSCAN profiles were not obtained for the sources it is not possible to assess the source structures. Comparison of the co-added centroid positions and maximum flux positions for each source in each band, however, suggests that many of the sources exhibit extension and are likely dominated by heating from external stars. At least 14 of the sources exhibit L_c(bol) $> 3L$(ext. htg.), however, and should be of interest for future study.

The last six sources in Table 2 are positioned in a region of obscuration immediately to the east of the visible H II region. The fact that the extended 60 μm emission (Fig. 1) in IC 1396 encompasses this region suggests that the obscuration is physically related to the complex.

3. ANALYSIS OF SOURCES

3.1. *The $R_{23} - R_{23}$ Color-Color Plot*

Wouterloot & Walmsley (1986) show that some discrimination among the character of YSOs is possible through a plot involving 25, 60, and 100 μm fluxes. Defining $R_{23} = \log(25S_{60}/60S_{25})$ and $R_{34} = \log(60S_{100}/100S_{60})$, a plot of the sources in Table 1 (*crosses*) and Table 2 (*circles*) is exhibited in

TABLE 2

ADDITIONAL *IRAS* SOURCES IN OR NEAR IC 1396

IRAS Source (1)	R.A.(1950) (*S*) (2)	Decl.(1950) (″) (3)	*S*(12) (Jy) (4)	*S*(25) (Jy) (5)	*S*(60) (Jy) (6)	*S*(100) (Jy) (7)	L_c(bol) (8)	L_c(ext. htg.) (9)
21304+5702C	27.8	48	0.27	0.40	5.3	33.9	31.4	20.9
21309+5711C	55.9	45	0.74	1.22	13.6	59.4	60.2	44.4
21310+5651	02.9	00	0.52	0.66	7.8	45.9	43.7	10.6
21334+5751C	24.7	39	0.35	0.40	5.9	49.4	43.9	10.3
21340+5734C	04.4	52	4.29	2.00	1.7	12.5	29.0	19.7
21342+5628C	17.5	41	0.23	0.37	4.1	19.5	19.4	8.4
21349+5801C	55.6	11	0.39	0.58	8.0	37.6	37.0	11.4
21361+5607C	06.1	56	0.26:	0.39	2.7	11.9	12.6	5.0
21382+5632	15.8	59	0.23	0.35	3.6	29.2	26.3	14.0
21397+5813	43.8	14	0.28	0.47	3.8	29.1	26.7	6.3
21400+5632C	01.8	30	0.33	0.49	8.4	43.0	41.1	10.5
21401+5614	11.0	34	0.35	0.42	2.4	17.2	16.8	5.5
21416+5612	37.0	48	0.80	1.10	8.0	24.0	28.9	4.7
21422+5625	12.6	05	0.43	0.34	6.2	31.6	30.9	6.3
21426+5723	41.4	51	0.19	0.27	4.4	15.2	16.1	12.6
21429+5634C	56.0	10	0.22	0.23	4.3	21.5	20.8	8.0
21436+5656C	38.7	51	0.23	0.53	5.9	20.9	22.1	9.0
21448+5633C	48.8	30	0.21	0.32	4.5	22.7	22.0	11.8
21467+5627C	45.9	48	0.33	0.40	3.2	23.8	22.3	3.7
21470+5655C	05.3	58	0.13	0.24	4.3	21.1	20.2	4.1
21472+5642	15.8	04	0.18	0.28	4.9	18.8	19.2	3.9
21477+5709	44.4	08	0.47	0.24	2.1	13.0	13.5	3.5
21480+5640	00.7	28	1.73	7.64	16.6	27.6	50.6	3.1
21481+5653	08.7	39	0.49	0.43	5.8	18.6	21.1	3.2

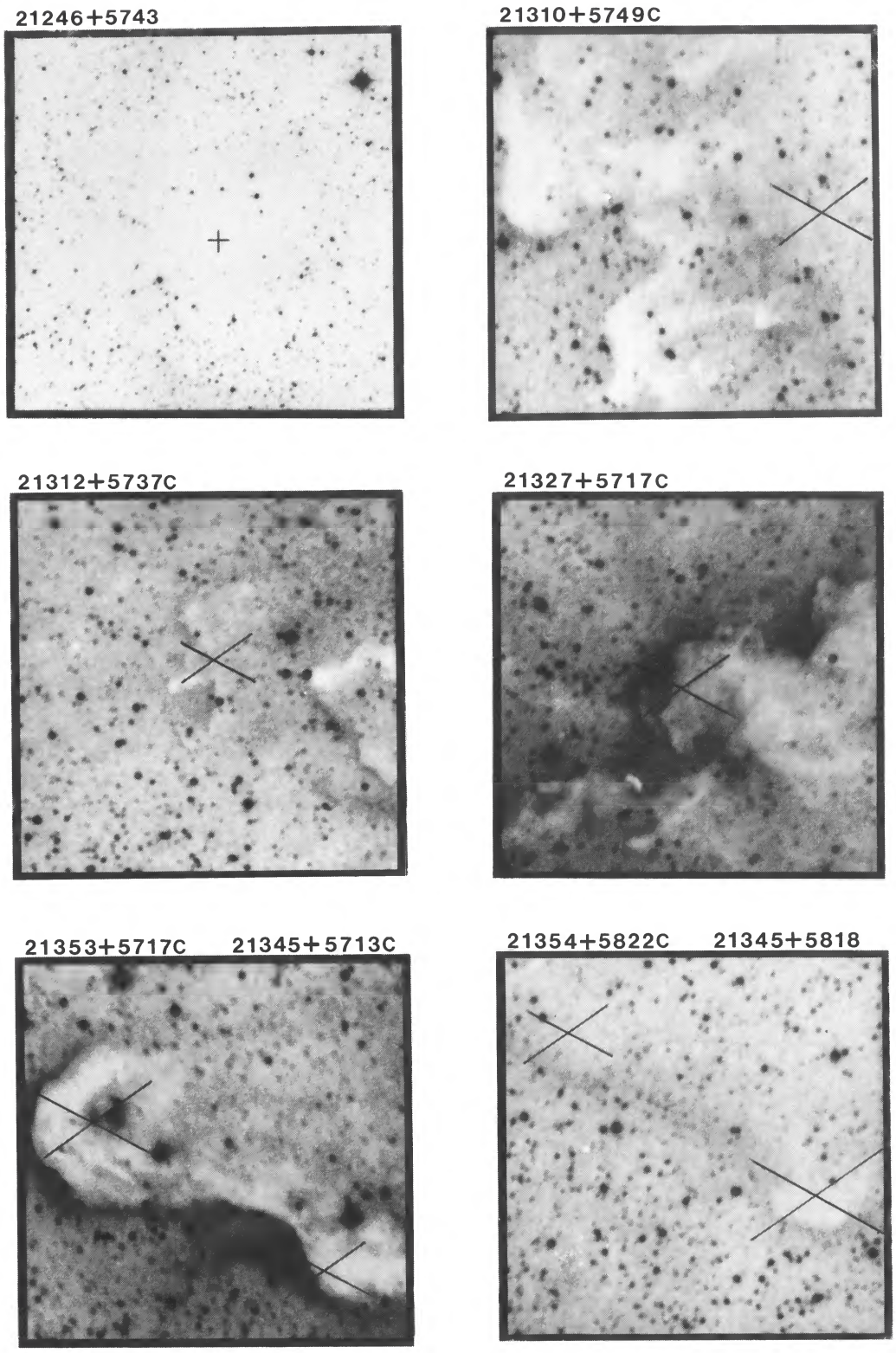

FIG. 4.—Finder charts for the *IRAS* sources in Table 1. All fields are 10′ on a side, except for 21246+5743 which is 20′ on a side. The fields have north up and east to the left, and have been reproduced from the E prints of the Palomar Observatory Sky Survey with permission of the Mt. Palomar Observatory.

PLATE 18

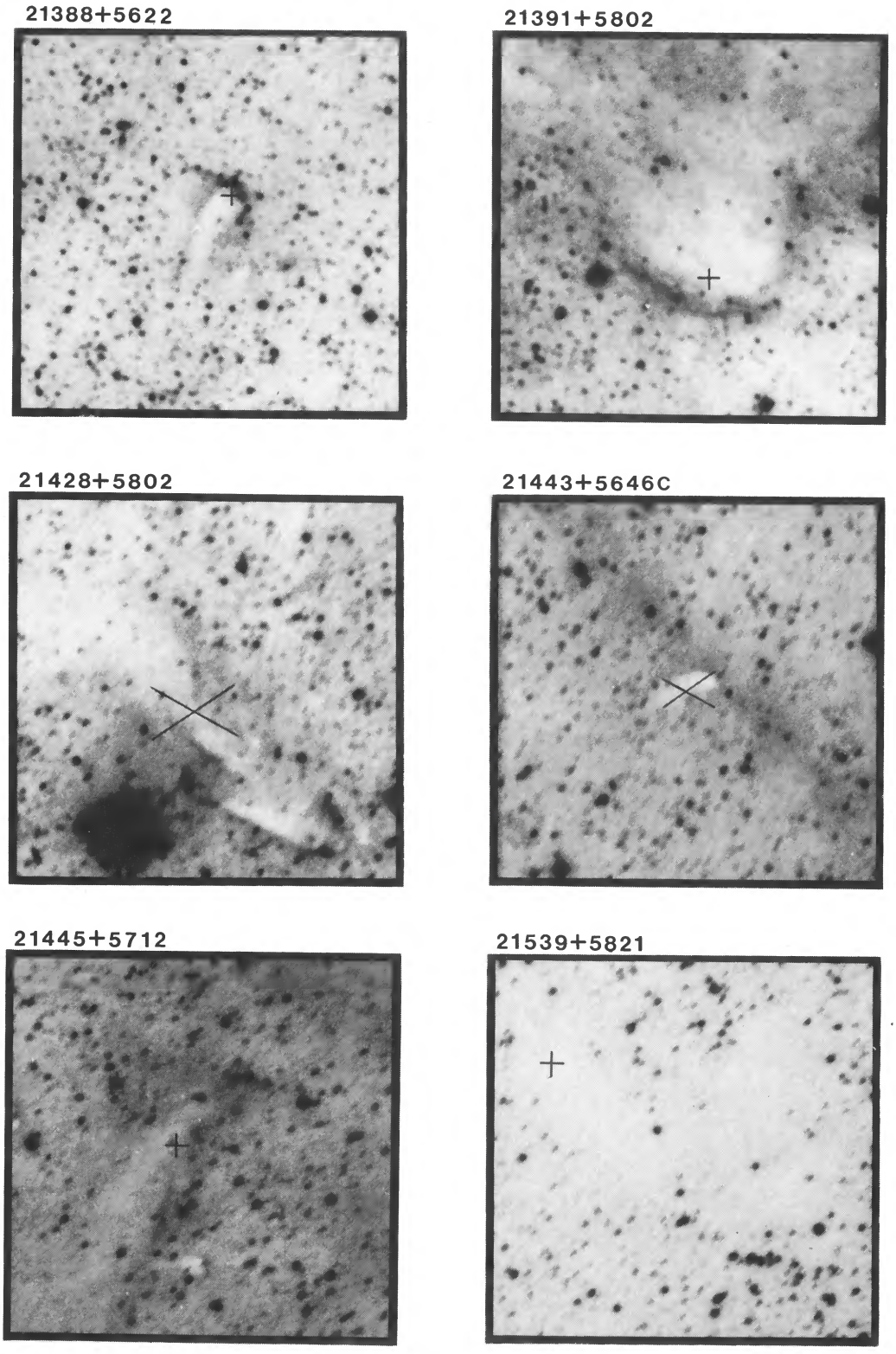

FIG. 4—*Continued*

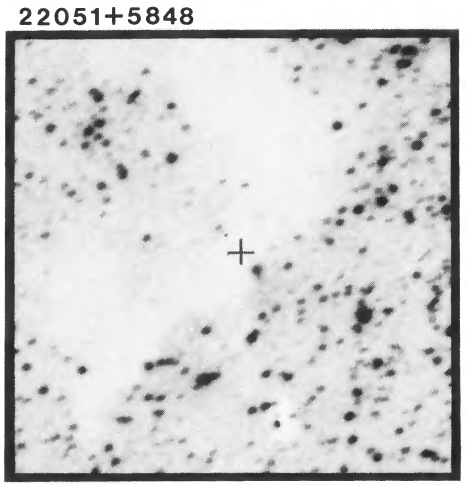

FIG. 4—*Continued*

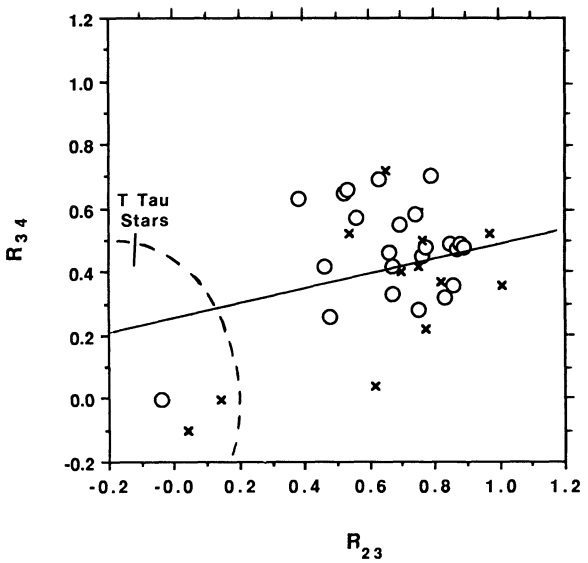

FIG. 5.—Color-color $R_{23} - R_{34}$ plot for sources in Table 1 (×) and Table 2 (○). The straight line separates H_2O sources (below the line) from a wider scatter of embedded sources according to Wouterloot & Walmsley (1986).

Figure 5. A line defined by $R_{34} = 0.261 + 0.227R_{23}$ is shown which, according to Wouterloot & Walmsley (1986), separates sources with H_2O maser emission (below the line) from a wider scatter of embedded sources without H_2O emission (i.e., not all sources below the line are masers). A region containing T Tauri stars is outlined on the left side of the diagram. We note that two of the sources in Table 1 (21388+5622 and 21445+5712) and one source from Table 2 (21480+5640) possess colors compatible with T Tauri stars. Most of the sources in Figure 5 are typical of deeply embedded objects. One of the embedded sources (21391+5802) is associated with a H_2O maser (see below), and indeed falls in the midst of H_2O maser color-color range seen in the plot of Wouterloot & Walmsley (1988). Assuming an emissivity proportional to frequency, the R_{23} color temperatures of the embedded sources in Figure 5 are in the range 50–80 K, and the R_{34} color temperatures are in the range 22–40 K.

3.2. *The Primary YSO Candidates*

Six of the sources in Table 1 exhibit pointlike structure and show L(bol) > 3L(ext. htg.), indicating that they are probably dominated by the presence of embedded YSOs. Additional observations are available for some of the objects as discussed below.

21246+5743. This source lies in an uncataloged dark cloud of unknown distance about 45′ west of the western bright rim of IC 1396. The cloud, about 6′ in diameter, has a faint centrally located nonstellar object visible on the red Palomar print. Within the positional uncertainties (±6″) of the *IRAS* source locations in Figure 4, 21246+5743 appears to be coincident with the nonstellar object. The source is positioned outside the IC 1396 coadded scan area, so the S_c fluxes in Table 1 refer to PSC fluxes. The absence of a 12 μm source detection indicates the possibility of a deeply embedded object, and it is not clear if this object could produce the observed semistellar nebulosity unless the nebulosity is a Herbig-Haro object produced by mass ejection from the YSO. Although the 25 μm ADDSCAN profile is somewhat noisy, the 60 μm profile appears as a well-defined point source. At 100 μm a prominent bump appears on the profile which could be caused by a very cold source about 3′ (NW or NE) from 21246+5743. As a consequence, the object is not a well-defined 100 μm point source as shown by the difference in the $S_c(100)$ and $S_s(100)$ fluxes in Table 1. Because few stars appear foreground to the globule, it is possible that the source is somewhat closer than 750 pc. Thus the estimated L(bol) range 30–90 $L_\odot$ is probably an upper limit, and the source could represent an intermediate mass embedded T Tauri star.

Observations of ^{12}CO (2–1) in the cloud by one of us (B. A. W.) indicate a temperature of $T_R^* \sim 12$ K with a FWHM of 5.2 km s^{-1} in a 28″ beam. The CO line profile has an apparent self-absorption feature located about 0.5 km s^{-1} to the red of the profile center, although this feature deserves confirmation since it could have been caused by a cold cloud in the reference beam. There is a hint of non-Gaussian wings on the profile which could signal the presence of mass outflow. Although the CO temperature is lower than that seen in other clouds with embedded YSOs, the temperature is a lower limit owing to possible beam dilution of a more compact source.

21388+5622. This source is located near the bright rim of GRS 12, a small opaque globule with dimensions 0.′7 × 2′. Although a very minor external heating contribution is suggested by the presence of faint wings on the ADDSCAN profiles (Fig. 3*c*), the source is evidently dominated by an internal heating source with a luminosity of ~155 $L_\odot$. With the luminosity of an A star and the far-IR colors of a T Tauri star, it is not clear if a single YSO with a substantial circumstellar shell is present, or if two or more unresolved YSOs may be contributing to the flux. Gyulbudaghian et al. (1990) have discovered an H_2O maser at the *IRAS* source position. The maser flux is 130 Jy at $v_{LSR} = -3.9$ km s^{-1}. Since masers are more common in luminous, deeply embedded objects, we suspect that a single YSO may be present. B. A. W.'s observation of ^{12}CO (2–1) yields $T_R^* \simeq 10$ K with FWHM ≃ 2.6 km s^{-1}. The ^{12}CO profile appears to be asymmetric with an enhanced blue wing at low velocity, possibly due to mass outflow. The low temperature and relatively narrow ^{12}CO line profile, however, are uncharacteristic of clouds which harbor more luminous YSOs. It is possible that this is a very young object which has yet to impart significant mechanical energy (via mass outflow) to the globule.

Most recently, Duvert et al. (1990) have reported ^{12}CO (1–0) and ^{13}CO (1–0) observations of this source at 20″ resolution, revealing a bipolar outflow, possibly emanating from an 18th mag star close to the *IRAS* source position. Also, with CS observations, the density structure of the globule is discussed.

21391+5802. This is the most luminous (~460 $L_\odot$) of the sources in Table 1 for which identification as a YSO is certain. At 12 μm the ADDSCAN profile is quite broad (~5′ at zero intensity), indicating warm dust emission from the globule as a whole. The COADD point source template fit at 12 μm is ill-determined. At 25 μm a broad (~5′) pedestal is still evident, but a prominent point source becomes evident, superposed upon the pedestal. The 60 and 100 μm profiles are dominated by point source-like emission, with faint broad wings extending especially to the north of the point source.

The CO (1–0) observations of Sugitani et al. (1989) first established 21391+5802 as an outflow source. The outflow has been confirmed through CO (2–1) observations by Wilking, Blackwell, & Mundy (1990). The ^{12}CO profile shows strong self-absorption with wings to −15 and +16 km s^{-1}, whereas the ^{13}CO shows a simple Gaussian profile (i.e., optically thin

emission). An interferometric map obtained in $C^{18}O$ (1–0) emission (Wilking & Mundy 1991, in preparation) with 7″ resolution shows an emission peak at the *IRAS* source location, with comparably bright emission extending 30″ to the southeast of the source. Another emission peak is seen about 18″ southwest of the *IRAS* position. It is not clear which, if either, of these extensions are associated with the mass outflow. Wilking & Mundy (1991, in preparation) have also detected CS (5–4) emission at the source position with $v_{LSR} = 0.28$ km s^{-1} and a FWHM $\simeq 3.4$ km s^{-1}. Continuum measurements at 2.73 mm (Wilking et al. 1989) show a prominent, unresolved source at the *IRAS* position, probably due to compact, cold dust. Gyulbudaghian et al. (1990) report detection of two H_2O maser lines at the source with fluxes of 9 and 35 Jy, respectively, at velocities of -5.2 and 2.7 km s^{-1}.

Wilking (1987, unpublished) has also mapped the immediate vicinity of 21391 + 5802 at 2.2 μm using an aperture photometer at the IRTF. Although no *H*, *K*, or *L* source was detected at the position of the *IRAS* source (which is consistent with an extrapolation of the *IRAS* fluxes), four near-IR sources were discovered close to the *IRAS* source. Table 3 gives details of the measurement on these sources, including positions and *H*, *K*, and *L* magnitudes. In addition, source *D* was detected at *N*(10 μm) with a magnitude 6.63 $\pm$ 0.3. It is not known if these are background sources or sources intrinsic to the cloud. Source *D* does possess $(K-L)/(H-K)$ colors indicative of a star with intrinsic infrared excess, whereas source A has colors which could be caused by interstellar reddening of a background star. It is possible that some or all of these near-IR objects are relatively low luminosity YSOs ($\leq 10\ L_\odot$) which, as a group, contribute to the extended emission seen in the *IRAS* bands at 12 and 25 μm. Near-IR source *D* appears to be coincident (within ± 6″) with a star located immediately inside the bright rim of GRS 14 about 55″ in position angle $\sim 110°$ from 21391 + 5802. The source locations are shown in Figure 6 which also displays the $C^{18}O$ map of Wilking & Mundy (1991, in preparation) and the position of 21391 + 5802.

21445+5712. The small globule GRS 29 (3′ × 0.′7) protrudes into the H II region on the eastern side of IC 1396. The source 21445 + 5712 is located near the center of the globule, and within the positional uncertainties it appears to be coincident with a faint ($m_r \simeq 18$) red star. This is one of the two sources in Table 1 with colors indicative of a T Tauri star, so it is reasonable to conclude that the source in question is a T Tauri star of moderate to high luminosity. At 12, 25, and 60 μm, the ADDSCAN profiles show prominent point source structure, with extended (1′–2′) pedestal emission from the globule at $\sim 5\%$ of the peak intensity of the source. At 100 μm, in addition to a probable point source there appears to be substantial extended ($\sim 4'$) emission, especially to the south of the source. This "excess" 100 μm emission is largely responsible for the greater value of L_s(bol) as compared with L_c(bol). The L_c(ext. htg.) for the COADD source is consistent with that seen in the pedestal emission, so the infrared source luminosity is estimated to be $\sim 100\ L_\odot$.

TABLE 3

NEAR-IR SOURCES NEAR 21391 + 5802

Source	α(1950)	δ(1950)	*H*	*K*	*L*
A.....	21^{h}39^{m}11.^{s}6	+58°02′37″	15.83	12.92	10.69
B.....	21 39 13.0	+58 02 25	13.61	12.57	
C.....	21 39 15.8	+58 01 57	12.92	12.50	
D.....	21 39 16.4	+58 02 21	13.07	11.48	9.92

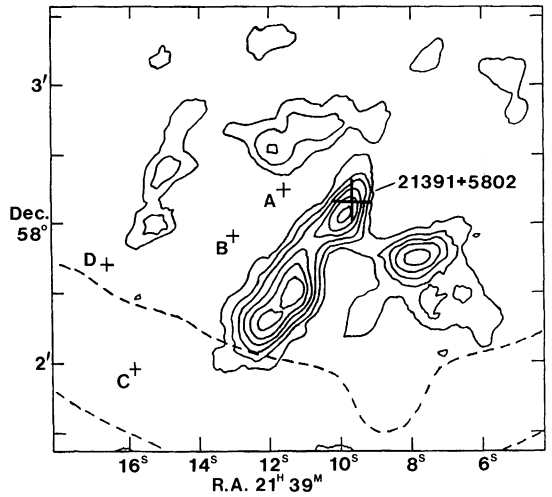

FIG. 6.—Sketch of the immediate vicinity of 21391 + 5802 located in GRS 14. The $C^{18}O$ interferometric mapping is represented by contours with integrated intensity levels of 0.4, 0.8, 1.2, 1.6, 2.0, and 2.5 Jy beam^{-1} km^{-1} s^{-1}, and the near-IR sources found by Wilking (Table 3) are located in the diagram. The bright rim of the globule is indicated by the region encompassed by dashed lines (see Fig. 4).

21539+5821. This source is located in LDN 1139 about 1° east of the eastern edge of IC 1396. The S_c fluxes in Table 1 are from the PSC. Although the distance to the dark cloud is unknown, a value of 750 pc has been used for the luminosity computations in Table 1. The ADDSCAN profiles show no hint of a source at 12 and 25 μm at the proper location, although a noisy peak at the 0.1 Jy level at both 12 and 25 μm appears about 1.′5 (SE or SW) of the 60/100 μm position. At 60 and 100 μm the source appears to possess well-defined pointlike structure. The absence of association with a visible object suggests that this source may represent a YSO in a very eary stage of evolution. The modest luminosity ($\sim 28\ L_\odot$ for a distance of 750 pc) indicates a possible pre–T Tauri object, and additional infrared and radio observations of the object are clearly in order.

22051+5848. Located in GRS 32 (= LDN 1165) about 2.′6 east of IC 1396, this object shows prominent point source structure at 25, 60, and 100 μm. Curiously, at 12 μm a pointlike source at about 1.7 Jy is located roughly 40″ to the NE or NW of 22051 + 5848, with the 12 μm ADDSCAN profile showing slight broadening indicating some contribution from 22051 + 5848. At 25 μm the 22051 + 5848 source dominates, with a faint wing on the ADDSCAN profile at the position of the 12 μm source. The 12 μm source may be associated with a faint star ($m_r \sim 18$) clearly seen in the photograph (Fig. 4) about 40″ northeast of 22051 + 5848. A brighter nebulous star is located about 30″ southwest of 22051 + 5848, and within the positional uncertainties it is possible that the *IRAS* source is associated with this object. As in the previous source, a distance of 750 pc was assumed for the luminosity calculations, and the S_c fluxes in Table 2 were drawn from the PSC. The globule GRS 32 has been observed by Gyulbudaghian et al. (1986) to show ^{12}CO emission. The measurement, however, probably excluded the *IRAS* source location since the telescope beam (2.′6) was centered in the southern portion of the globule at a declination of 58°45.′6. The CO velocity (-1.64 km

s^{-1}) indicates that the globule may be part of a foreground system of globules (the BD+55 2612 system), and thus the assumed distance of 750 pc and luminosity ($\sim 120\ L_\odot$) should be regarded as an upper limit.

3.3. *Comments on Other Globule Sources*

21310+5749C. The ADDSCAN profiles are broad with an indication of four sources at 12 and 25 μm located within 2′ of the primary position. The photograph indicates a source location in a somewhat diffuse area of obscuration, clearly outside of the most heavily obscured regions of the GRS 3 complex. Because of the complicated source profile structure, the COADD fluxes are ill-determined at the primary source position as indicated in Figure 3*b*.

21312+5737C. Most of the flux in this source can probably be attributed to external heating as indicated by the profile width correspondence to the size of the globule ($\sim 2'$, see Fig. 4) and the rough equivalence of L_s(bol) and L_s(ext. htg.). The ADDSCAN did pass through the position of the PSC source 21306+5733, and the 21312+5737C profile is partially blended with 21306+5733. The source IRAS 21306+5733 lies about 5′ southeast of 21312+5737C in a region without obvious cloud structure. The co-added survey did not detect 21306+5733 at 100 μm.

21327+5717C. This source is located just inside the leading edge of a bright-rimmed globule (GRS 4) also designated as Pottasch B1 in the H I observations of this region by Matthews (1979). The ADDSCAN profiles exhibit structure which could be interpreted either as three blended sources (one about 1′ SE or SW of the central peak with $\sim 60\%$ central peak intensity, and one about 1.′5 NE or NW of the central peak with about 40% central peak intensity), or as the effect of extended cloud structures. At 60 μm and especially at 100 μm the resolution is insufficient to reveal the structure seen at 12 and 25 μm, and the 100 μm profile width of $\sim 4'$ is characteristic of the size of the globule. Because of the source complexity, the COADD fluxes are not well-determined. The prominent excess of L(bol) over L(ext. htg.) for both the COADD and SCANPI estimates, however, suggests that this region deserves additional infrared and radio observations at higher spatial resolution.

21345+5818. Located at the middle of the small bright-rimmed globule GRS 5, this source has many similarities to 21327+5717C. The 12 and 25 μm ADDCAN profiles show structures with two peaks separated by $\sim 2'$. The broad profiles in all bands almost certainly arise from global external heating of the globule. The COADD fluxes are poorly determined, and infrared observations at higher spatial resolution will be required to discern if any point sources are present in the globule.

21345+5713C. This source shows a peak intensity near the inside edge of bright-rimmed globule GRS 6 (= Pottasch A2, see Matthews 1979). The ADDSCAN profile exhibits a very sharp gradient in all bands across the bright rim (see Fig. 3), with extended structure matching the visible extent of the globule. Like the previous two sources, the COADD fluxes are poorly determined, and the external heating estimate suggests that the source is due entirely to external heating.

21353+5717C. With a broad structured profile and proximity (3.2 pc projected distance) to HD 206267, this source is almost certainly dominated by external heating. Located in the prominent globule GRS 6 (= Pottasch A1, see Matthews 1979), the 100 μm peak position is located $\sim 40''$ east of the star LkHα 349, a late F star obscured by 3.9 mag of extinction (Dibai 1969) and which is probably interacting with the globule. Indeed, the ADDSCAN profiles which partially intersect the stellar position show small peaks at 12 and 25 μm at the position of the star. de Muizon et al. (1980) carried out far-IR scans of this globule with a 4.′5 beam, concluding that a 5000 $L_\odot$ B1 or B2 star is embedded essentially at the position found by our COADD survey (Table 1). The *IRAS* scans, however, suggest that the de Muizon et al. (1980) luminosity estimate is high, and that no source intrinsic to the globule is required (except perhaps a minor contribution from LkHα 349). This bright-rimmed globule has been studied in H I (Matthews 1979) and CO (Wootten et al. 1983), the latter of which shows no indication of an unusual CO velocity dispersion which might be expected if the globule contained a B star.

21354+5822C. Situated in a small globule (LDN 1116) about 6.′5 northeast of GRS 5, this source exhibits a near point-like ADDSCAN profile superposed upon an extended ($\sim 4'$) region at 12 and 25 μm. At 60 and 100 μm the profile broadens with the rise of the pedestal which presumably represents an external heating contribution. A faint, elongated nebular object is visible immediately to the southeast of the *IRAS* position, and it is possible that an embedded source is present at or near the object. Because of the irregular source profiles, however, the COADD fluxes are not well determined, and the interpretation remains ambiguous.

21428+5802. This source is associated with a dust lane extending to the northeast from GRS 20. The width of the ADDSCAN profiles is comparable to the width of the dust lane. With ill-determined COADD fluxes, the source may consist entirely of externally heated dust.

21443+5646C. The globule GRS 23 is a small (0.′5 × 2′) opaque dark cloud in the southeastern region of IC 1396. With non-point source profiles and the probability of adequate heating by external stars, it is unlikely that this source contains an embedded object.

4. SUMMARY

We have identified six globule-related *IRAS* sources located in or near IC 1396, which probably represent YSOs in various stages of evolution. Two of the sources (21388+5622 and 21445+5712) show colors indicative of T Tauri stars. Another source, 21391+5802, is the most luminous of the objects studied. Radio studies indicate that this deeply embedded source has already developed an outflow, and additional observations, for example, of the H_2 emission in the region, would be useful for clarification of source morphology. Three sources are located in dark clouds outside the immediate IC 1396 H II region, and may represent YSOs in very early stages of evolution. A number of additional sources are discussed, and the combination of resolved source profiles and the possibility of substantial external heating from OB stars in the complex indicates that the bulk of these sources do not contain YSOs. A second list of 24 sources which are not associated with globules contains a number of sources with luminosities suggestive of intrinsic heating. In particular, six of the sources are located in a region of obscuration at the SE edge of IC 1396 and are good candidates for additional study.

We wish to thank the Image Processing and Analysis Center (IPAC) for support in the data analysis. This research was supported in part by NASA grant NAG 5-1157 to the Uni-

versity of Missouri-St. Louis through the Astrophysics Data Program. One of us (R. D. S.) acknowledges support from NSF grant AST 8813917 and a Chrétien Award from the American Astronomical Society. A. L. G. acknowledges support as a Visiting Scholar to the University of Missouri, St. Louis under auspices of the Center for International Studies.

REFERENCES

Balázs, L. G., & Kun, M. 1989, Astr. Nach., in press
Chavarria, K.-C. 1981, A&A, 101, 105
Cohen, M. 1973, MNRAS, 164, 395
———. 1990, ApJ, 354, 701
de Muizon, M., Rouan, D., Léna, P., Nicollier, C., & Wijnbergen, J. 1980, A&A, 83, 140
Dibai, E. A. 1969, Astrofizica, 5, 249
Draine, B. T., & Anderson, N. 1985, ApJ, 292, 494
Duvert, G., Cernicharo, J., Bachiller, R., & Gómez-González, J. 1990, A&A, 223, 190
Emerson, J. P. 1988, in "Formation of Low Mass Stars." Proceedings of the NATO Advanced Study Institute, ed. A. K. Dupree & M. T. V. T. Lago (Dordrecht: Reidel), p. 21
Gyulbudaghian, A. L. 1985, Astrofizica, 23, 295
Gyulbudaghian, A. L., Rodriguez, L. F., & Canto, J. 1986, Astrofizica, 24, 201
Gyulbudaghian, A. L., Rodriguez, L. F., & Curiel, S. 1990, Rev. Mexicana Astr. Af., 20, 51
IRAS Point Source Catalog, Version 2. 1988, prepared by G. Helou & D. Walker (Washington, DC: GPO)
IPAC User's Guide 1989, Edition 4 (Pasadena: California Institute of Technology)
Kun, M. 1986, Ap&SS, 125, 13
Kun, M., & Balázs, L. G. 1987, Publ. Astron. Inst. Czech. Acad. Sci., 69, 161
Kun, M., Balázs, L. G., & Toth, I. 1987, Ap&SS, 134, 211
Lynds, B. T. 1962, ApJS, 7, 1
Marschall, L. A., Comins, N. F., & Karshner, G. B. 1990, AJ, 99, 1536
Matthews, H. E. 1979, A&A, 75, 345
Olnon, F. M., Baud, B., Habing, H. J., de Jong, T., Harris, S., & Pottasch, S. R. 1984, ApJ, 278, L41
Osterbrock, D. E. 1957, ApJ, 125, 622
Pottasch, S. R. 1956, Bull. Astr. Inst. Netherlands, 13, 77
Simonson, III, S. C. 1968, ApJ, 154, 923
Simonson, III, S. C., & van Someren Greve, H. W. 1976, A&A, 49, 343
Sugitani, K., Fukui, Y., Mizuno, A., & Ohashi, N. 1989, ApJ, 342, L87
Wilking, B. A., Blackwell, J. H., & Mundy, L. G. 1990, AJ, 100, 758
Wilking, B. A., Mundy, L. G., Blackwell, J. H., & Howe, J. E. 1989, ApJ, 345, 257
Wootten, A., Sargent, A., Knapp, G., & Huggins, P. J. 1983, ApJ, 269, 147
Wouterloot, J. G. A., & Walmsley, C. M. 1986, A&A, 168, 237